A tree-ring based reconstruction of early summer precipitation in southwestern Virginia (1750-1981)

Andria Dawson*
347 Evans Hall
University of California, Berkeley
Berkeley, CA
94720
andria.dawson@gmail.com

David Austin
Department of Geography
University of North Alabama
Florence, Alabama
35632

David Walker
Department of Forest Resources and Environmental Conservation
Virginia Tech
Blacksburg, VA
24061

Sarah Appleton
Department of Geography Society and Environment
University of Minnesota
414 Social Sciences
267 19th Ave S
Minneapolis, MN
55455

Bronwyn Gillanders
Southern Seas Ecological Laboratories
Darling Building DX 650 418
School of Earth & Environmental Sciences
University of Adelaide SA 5005Australia

Shelly M Griffin
Department of Geological and Atmospheric Sciences

Iowa State University
Ames, Iowa
50011

Chika Sakata
California State University
Dominguez Hills
1000 E. Victoria St.
Carson, CA
90747

Valerie Trouet
Laboratory of Tree-Ring Research
University of Arizona
Tucson AZ
85701

October 23, 2014

Abstract

In a closed-canopy forest, stand dynamics play an important role in shaping the forest, and it has been hypothesized that dense forests are not sufficiently limited by climate to warrant climate reconstruction. We collected *Quercus prinus* tree-ring data from a dense forest in the Appalachians, and after removal of stand dynamics and age trends we found strong correlations between annual tree growth and early summer precipitation. To strengthen the climate signal, we include additional southeastern US *Quercus prinus* chronologies in a nested principal component analysis (PCA). Correlation between the growth proxy and early summer precipitation was increased through PCA, and assessment of reconstruction skill was favorable. Our May-June precipitation reconstruction was modeled using Bayesian regression, which allowed uncertainty to be quantified. The reconstruction covered the period 1750-1981, and extended the instrumental record by 150 years. It also showed key drought years identified by other regional reconstructions, as well as an 11-year periodicity, possibly related to solar variability. This reconstruction establishes a baseline precipitation record that can be used to measure changes brought about by global climate change.

Keywords: reconstruction, precipitation, Virginia, tree rings, climate, principal components, forest, dendrochronology

1 Introduction

Global circulation models project an increase in average global surface temperatures of 1.0 - 3.5 ° C by the end of this century due to continued increases in greenhouse-gas emissions (IPCC 2013). However the influence of increased radiative forcing on precipitation regimes is not well understood, and this is particularly the case for the southeastern United States (US). The 24 models used to make predictions about climate change in the Intergovernmental Panel on Climate Change Fourth Assessment Report were not in consensus with respect to drought frequency in this region (IPCC 2007, Seager et al. 2009). Uncertainty in climate projections makes it difficult to predict water usage. The ability to do so is crucial because the southeastern US has experienced substantial increases in population and energy consumption over the last decade (Seager et al. 2009, Sobolowski et al. 2012). Recent droughts have had major socioeconomic impacts as a result of devastation to both agriculture and crop production (Wang et al. 2010). To deal with these issues, it is important that both urban and water planners in the southeast have access to information regarding climate change projections and mitigation. Through the use of tree-ring based climate reconstructions, we can better understand past precipitation regimes at both decadal- and centennial time-scales, improving projections of future precipitation patterns.

In order to reduce uncertainty in climate model projections and to extend meteorological records further back in time, tree-ring data are commonly used as regional proxies, particularly in regions where drought (e.g. the American Southwest, Cook et al. 2004) or summer temperature (e.g. the European Alps, Büntgen et al. 2007) is the limiting tree growth factor. Tree-ring data have also successfully been used for climate reconstructions in temperate climate regions characterized by high humidity such as the eastern US (LeBlanc 1993, Stahle et al. 1993, Cook et al. 1999). Tree growth in these regions is typically less sensitive to drought variability than trees in semiarid regions (Phipps 1997). The amount of environmental variability recorded in tree-ring time series from a certain area

thus generally depends on the degree to which environmental factors are limiting tree growth in that area (Fritts 1976). Furthermore, it is traditionally understood that trees in a closed-canopy forest are not limited by climate to the same extent as trees growing on the forest border. Within a dense forest, stand dynamics play an important role in shaping the forest structure through their influence on radial tree growth and tree survival. As these interactions between individuals increase in strength, the climatic influence on tree growth becomes less dominant.

Despite these challenges to capturing a strong climate signal in tree-ring time series from southeastern US forests, numerous studies have identified significant climate-growth relationships (Pan et al. 1997, Speer et al. 2009, Rubino & McCarthy 2000) and several tree-ring based precipitation reconstructions have been developed for the southeastern US. The most prominent of these reconstructions is likely a spring rainfall reconstruction for the past 1000 years based on Bald cypress (*Taxodium distichum*) tree-ring chronologies from North Carolina, South Carolina, and Georgia (Stahle & Cleaveland 1992). Bald cypress trees grow in excessively wet swamps, yet tree growth is strongly positively correlated with spring and early summer precipitation. At drier sites in Virginia, Pan et al. (1997) demonstrated for four deciduous species that both annual ring-width and basal area increments were positively correlated with precipitation from the prior summer and autumn, and current summer. They also report negative correlations with air temperature of the current growing season. Speer et al. (2009) found similar correlations between precipitation and temperature and annual tree growth for oak chronologies from closed canopy forests in the Southern Appalachian Mountains.

In this study, we determine the presence of a significant relationship between chestnut oak (*Quercus prinus*; QUPR from here on) annual growth series in the southern Appalachian Mountains and early summer precipitation and develop a regional QUPR tree-ring chronology. We then use the QUPR chronology to reconstruct early summer precipitation using Bayesian methods. Finally, we evaluated

the reliability of the reconstruction by comparing it to other verified regional climate reconstructions.

2 Materials and Methods

2.1 Tree ring data

The study site is an Upland Oak-Pine forest located on the north facing slope of Brush Mountain in Southern-West Virginia (37 ° 22.2' N, 80 ° 14.8' W), with a site elevation of 558 m (BM in Figure 1). This region is classified as either humid continental or mountain temperate, and characterized by warm, humid summers and winters that are predominantly cool with intermittent warm spells. The mean annual precipitation (1901-2010) at the nearby Blacksburg weather station is 1073 mm and the mean annual temperature is 10.9 ° *C*.

The study site supports dominant QUPR trees amongst a canopy of many species, including scarlet oak (*Quercus coccinea*), northern red oak (*Quercus rubra*), red maple (*Acer rubrum*), Virginia pine (*Pinus virginiana*), pitch pine (*Pinus pungens*), and eastern white pine (*Pinus strobus*). Site access was adjacent to the Appalachian trail but the site was selected to minimize human interference. The steepness of this slope suggested that climate may be a limiting growth factor, but the closed canopy and stand density suggested that stand dynamics may also play a significant role in shaping the forest structure (Fritts 1976).

We sampled 56 QUPR trees and collected two increment cores per tree. Samples were dried, mounted, and sanded according to standard procedures (Stokes & Smiley 1996). Crossdating was performed based on the list method, which makes use of marker years that signify relatively favorable or unfavorable growth years in a stand (Yamaguchi 1991). All samples were measured using a LINTAB measurement stage with 0.01mm precision, and visual crossdating was checked using COFECHA software (Holmes 1983). We used inter-series correlation, a measure of stand-level signal, and mean

sensitivity, to select a total of 76 tree-ring series from 53 trees to be used for site chronology development.

Non-climatic age and stand dynamics related trends were removed from the individual tree-ring series using smoothing splines with a 50 % cutoff at 50 years using ARSTAN software (Cook & Peters 1997). This method allowed us the flexibility to remove the episodic-like interaction effects from the time series, while retaining the high-frequency climatic variability. Note that as with any filtering technique, inevitably some portion of the climatic signal will be lost through the removal of these non-climatic trends (Cook & Peters 1981).We assume that the loss of climatic signal was negligible, and comparison of the detrended time series with climatic data ultimately determined if the strength of the remaining signal was sufficient to perform further analyses. The Brush Mountain site chronology was then calculated by averaging the individually detrended series using a biweight robust mean (Cook and Peters 1997), and will hereafter be referred to as BM.

We computed the expressed population signal (EPS) to measure the common variability in our chronology at an annual resolution. EPS depends on both signal coherence and annual sample-depth, and EPS values that fall below a predetermined cutoff (0.85) indicate that the chronology is not dominated by a coherent signal, and is therefore deemed less than ideal for climate reconstruction (Wigley et al. 1984) .

2.2 Principal component analysis

Water availability may not be the primary limiting factor to tree growth in southeastern US sites, but a large sample size may be sufficient to compensate for this effect and help to identify the common climate signals despite site and individual variability. In regions that are subject to site heterogeneity, where significant climatic variance cannot be identified for a standard sample size, principal component analysis (PCA) can be an effective means to extract the common signal in multiple sites

and thus overcome the lack of strength of climate signal in individual sites (Peters et al. 1981, Anchukaitis et al. 2006, Jacoby et al. 1989). Through the application of PCA, tree-ring data collected from a network of regional sites can be combined to reduce site level noise through the identification of a common climate signal across sites.

To increase the strength of the precipitation signal in our chronology, we combined the BM chronology with four eastern US *Quercus* chronologies (3 QUPR and 1 *Quercus alba*) in a nested singular value decomposition PCA (Wold et al. 1987, Cook et al. 2007; Table 1, Figs. 1 and 2). These four chronologies extended back to at least 1845 (the length of the BM chronology) and were significantly correlated with regional precipitation anomalies (see below). Tree-ring data for the four *Quercus* sites were downloaded from the International Tree-Ring Database (ITRDB; http://www.ncdc.noaa.gov/paleo/treering.html) and individual ring-width time series were detrended using a smoothing spline with 50% cutoff at 50 years (Cook & Peters 1981), and subsequently used to develop site chronologies. Chronology reliability for each of the four chronologies was assessed based on the mean sensitivity, inter-series correlation, EPS, and the first-order autocorrelation.

We applied a nested PCA approach to make use of the chronologies that extended prior to 1845: we combined the BM chronology with all four *Quercus* chronologies in a first PCA run (PCA_{1845}) and then added a second PCA run (PCA_{1750}) that included only the 3 chronologies that extended back to 1750 (LH, WD, and OC). For each PCA run, the PCA1 axes explaining the largest amount of common variance were retained for further analysis and were included in a climate correlation analysis. PCA_{1845} and PCA_{1750} resulted in two potential reconstructions each with its own set of skill and accuracy statistics, as described in section 2.5. We merged the two reconstructions at the year 1845 (1845-1981 from PCA_{1845} and 1750-1844 from PCA_{1750}) for the final SWV (for southwest Virginia) chronology. We highlight that the BM chronology is determined for a single point, but that the SWV

chronology is representative of the climate in the surrounding region as a result of being constructed from a PCA on growth series from sites spatially distributed around this point.

2.3 Climate data

We applied a two-tier approach to select the optimal climate target for reconstruction. In a first step, we used monthly climate values from the Blacksburg climate station (37 ° 12' N, 80 ° 24' W; elevation 634 m; 1901-2006) in a correlation function analysis with BM chronology. For this purpose, monthly precipitation sums and average temperatures and Palmer Drought Severity Index (PDSI) values were computed from daily measurements. Pearson's correlation coefficients were calculated for all months starting in April of the year previous to the growing season through current December, as well as for various seasons (Apr-June, July-Sep, Oct-Dec, Jan-Mar) and annual means. This analysis showed that the BM chronology was most strongly correlated with average May and June precipitation ($r=0.53$, $p<0.01$).

This result was then used in a second step as guidance for a spatial correlation analysis between the SWV chronology and a gridded (0.5 ° × 0.5 °) monthly climate data set for the period 1901-2006 [CRUTS3.10; Harris et al. 2014]. Spatial correlations were calculated using the KNMI climate explorer [http://climexp.knmi.nl; Trouet & van Oldenborgh 2013]. The grid point showing the strongest correlation between the SWV chronology and May-June precipitation was then selected as a target for further climate-growth analysis and for reconstruction.

2.4 Reconstruction methods

Precipitation was modeled using a Bayesian linear regression model, with the first PCA chronology (1750-1981) as a predictor. The precipitation model is written as

$$y_t \sim Normal(\mu_t, \sigma^2) \quad (1)$$

$$\mu_t = \beta_0 + \beta_1 x_t, \quad (2)$$

where y_t represents precipitation values for the identified grid cell and x_t is the first PCA value at year t. Uninformative priors were placed on all three parameters as follows: $\beta_i \sim$ Normal(, 1000), and $\sigma^2 \sim$ Uniform(0, 100). Posterior distributions for all three parameters (β_0, β_1, and σ^2) were sampled using an adaptive Markov Chain Monte Carlo (MCMC) algorithm with a Metropolis step method, in which proposal distributions were adjusted accordingly when acceptance rates fell outside the ideal range of 0.2-0.5. The algorithm was run for 100,000 iterations with a burn-in of 50,000. Parameter estimates were thinned so that only every tenth estimate was saved. The 0.025, 0.5 and 0.975 quantiles of these estimates were determined to define an upper and lower bound for a 95% credible interval, as well as the median. At each iteration, parameter estimates were used to compute estimated precipitation. A 95% predictive interval was computed from these precipitation estimates using the 0.025, 0.5 and 0.975 quantiles. Note that frequentist methods could have been used with similar results, but we preferred the simple interpretation of the Bayesian credible interval.

2.5 Model calibration and verification

To assess the accuracy of the modeled precipitation anomalies, we used a split-period (1901-1941 and 1941-1981) calibration/verification scheme. Both the 1901-1940 and 1941-1981 periods of climate data were used in turn as the calibration period (denoted by y_t in 1), to determine if the accuracy of the reconstruction was sufficient to warrant further analysis. Data from the period not used for calibration served as verification data, and for both calibration/verification pairs we computed the mean squared error (MSE), reduction of error (RE) (Fritts 1976), coefficient of efficiency (CE) (Cook et al. 1994),

and the squared correlation (r^2) (See the National Research Council report Surface Temperature Reconstructions for the Last 2,000 Years (North et al. 2006) for further details on assessing reconstruction skill).

2.6 Reconstruction analysis

We compared our precipitation reconstruction to six published regional precipitation and drought reconstructions based on tree-rings as external validation (Table 2). One drought reconstruction was obtained from the North American Drought Atlas (NADA) (Cook et al. 1999), agridded reconstruction of PDSI values for June through August over the last 2,000 years. The second drought reconstruction was a July PDSI reconstruction (JT) for Virginia and North Carolinian coastal regions (Stahle et al. 1998). The next set of reconstructions were precipitation reconstructions for the North Carolina (NC), South Carolina (SC), and Georgia (GA) regions for the months of April though June for NC, and March through June for SC and GA (Stahle & Cleaveland 1992). The final reconstruction for early summer anomalies for the Montpelier region (MP) was based on tree-rings as well a meteorological diary (Druckenbrod et al. 2003).

Reconstructions that were significantly correlated with our reconstruction were compared using 31-year window running correlations, which facilitated the identification of periods of pattern dissimilarity.

Furthermore, we used a spectral wavelet analysis to identify dominant cyclical behavior in our reconstruction (Torrence & Compo 1998). Spectrum values were averaged with 2 frequencies per bin to simplify interpretation.

3 Results

The BM chronology covered the period 1764-2010 CE, had an interseries correlation of 0.556, and a mean sensitivity of 0.208 (Table 1). The EPS was higher than 0.85 for 1845-1981 and we thus used the chronology over this period. A spatial correlation analysis between climate variables and BM identified the grid point 37.5 - 38 ° N, 80.5 - 81 ° E as the location that correlated most strongly with our chronology (Fig. 3). The BM chronology was significantly positively correlated with monthly PDSI values from April of the previous year to December of the current year (Fig. 4B), except for previous May and previous October. We found particularly strong correlations between BM and monthly PDSI over the May through August growing season, with the highest correlation being with average June and July PDSI (jjPDSI; $r = 0.55$, $p < 0.01$). Furthermore, we found significant, positive correlations with precipitation of the previous year June and current year May and June (Fig. 4A). When averaging monthly precipitation values over the months May and June (mjPR), correlation increased to $r = 0.5$ ($p < 0.01$). The BM chronology did not correlate with monthly temperature values (Fig. 4C).

Based on this climate-growth analysis, mjPR and jjPDSI were considered as candidate targets for reconstruction. An assessment of the calibration/verification statistics for a reconstruction based on the BM chronology alone (results not shown), however, suggested that the climate signal was not sufficient to warrant adequate reconstruction skill. We therefore combined the BM chronology with four existing oak chronologies from nearby sites (Fig. 1, 2) in a nested PCA approach. All four chronologies were significantly positively correlated with the mjPR and jjPDSI values from the monthly data set obtained from the spatial correlation analysis (mjPR r: 0.38-0.55; jjPDSI r: 0.48-0.59; see Table 1).

The first PC axis ($PC1_{1845}$) of PCA_{1845} explained 57% of the common variance, with the second axis

explaining 15.2%. All oak chronologies had a positive loading on $PC1_{1845}$, thus reflecting the correspondence between the time series. PC1 of the PCA_{1750} run ($PC1_{1750}$) explained 56% of the common variance and $PC2_{1750}$ explained 28.3%. $PC1_{1845}$ and $PC1_{1750}$ were strongly positively correlated over the period of overlap ($r = 0.93$, $p < 0.001$) and we merged the PC1 time series at the year 1845 (PCA_{1750}: 1750-1844, PCA_{1845}: 1845-1981) to form a single chronology extending from 1750 to 1981. When comparing SWV with monthly climate variables, we generally find higher correlations than for the individually contributing tree-ring series (Fig. 3) and this is particularly true for mjPR ($r = 0.61$, $p < 0.01$) and jjPDSI ($r = 0.63$, $p < 0.01$). We thus tested mjPR and jjPDSI as potential reconstruction targets in a split calibration/verification scheme (Table 3). RE and CE values were negative for jjPDSI when using the later calibration period (1942-1981), indicating a poor fit of the reconstruction model. RE and CE are key statistics to determine the skill of a reconstruction, and our decision to reconstruct mjPR rather than jjPDSI was based on these values. Our final mjPR reconstruction, now referred to as rSWV, was scaled against the entire 1901-1981 interval. Estimates of rSWV and corresponding 95% predictive intervals were computed for each year of the period of reconstruction using posterior parameter draws (Fig. 5).

We compared rSWV to other regional moisture reconstructions (Table 4) and found positive correlations across the board. The strongest correlation was found with the NADA summer drought reconstruction ($r = 0.53$, $p < 0.01$), but we note that the LH chronology was used in the construction of both rSWV and NADA, thus implying that these records are not completely independent. A spectral analysis shows a periodicity in the rSWV reconstruction with peaks at 11, 17, and 24 years (Fig. 6).

4 Discussion

We investigated the relationship between climate and annual radial QUPR growth at a closed canopy site in the southeastern US. After removing the portion of the signal attributed to stand dynamics and

intrinsic age trends, we found that early summer (May through June) moisture was the strongest positive influence on radial growth. Similar climate-growth relationships have been identified by previous studies on oak in the southeastern US (Speer et al. 2009, Li 2011) and can be explained by ecophysiological mechanisms. Radial growth of oak species typically starts in April or May after leaf-out and is 90% complete by the end of July even in years with adequate moisture (Robertson 1992). In the first months of the growing season, carbon is allocated predominantly to radial thickening, whereas later in the season the focus of this allocation is shifted to carbohydrate storage (Zweifel et al. 2006). Under severe moisture stress, oak carbon allocation is shifted from shoot to root, thereby increasing the root/shoot ratio (Dickson et al. 1996). QUPR is considered to be more tolerant to drought stress than other oak species and exhibits several morphological adaptations in order to better cope with moisture stress events (Dickson et al. 1996). However, we found that its radial growth was strongly influenced by moisture availability, suggesting that in years with inadequate moisture, radial growth is not a priority and carbon allocation is likely focused on maintenance or root development. The identifiable moisture response in the detrended BM chronology demonstrates that oaks in a closed-canopy forest can be used as paleoclimate proxies if the non-climatic portion of the low-frequency signal in the tree-ring time series is removed with great care (Cook 1985, Cook et al. 1990). The development of a biologically motivated trend removal algorithm may improve current practices in dendroclimatology (Melvin & Briffa 2008). In addition, care must be taken in closed canopy forests when attempting to use growth series as proxy records as younger stands in the stem-exclusion phase may be dominated by the effects of competition rather than of climate (Oliver 1980).

To isolate and strengthen the moisture-growth relationship of the BM chronology, we performed a nested PCA including five regional summer moisture sensitive *Quercus* chronologies. The spatial pattern of the relationship between the resulting SWV chronology and early summer precipitation indicates that SWV is positively correlated with moisture in the Great Appalachian Valley (Figure 3).

Mountains play an important role in the hydrological cycle for several reasons, one of which being that they are the points of origin of most rivers (Beniston 1997). Increases in precipitation in mountainous regions leads to increased stream flow volumes and surface runoff, which in turn increases soil moisture in the Appalachian watershed.

Our reconstruction generally shows similar variability as other reconstructions of moisture variability in the southeastern US (Table 4). The strongest similarity was found with the NADA PDSI reconstruction (Figure 7), but we note the lack of full independence between these two records. Despite the overall strong agreement between both records, a 31-year windowed correlation between rSWV and NADA PDSI indicated that these records were not consistent for the period 1853-1866.

All five chronologies contributing to SWV show a pattern of reduced correlation with the NADA PDSI reconstruction during this period, which coincides with La Niña conditions occurring from 1855-1863 (Cole et al. 2002). La Niña events typically have strong impacts on the West Coast, but affect weather patterns throughout North America, and have even been shown to affect the Atlantic hurricane season (Pielke et al. 1999). During this large-scale ocean-atmosphere phenomenon, temperature anomalies in the southeastern US (National Oceanic and Atmospheric Administration 2014) in combination with low moisture availability likely led to a change in the otherwise stationary precipitation-growth relationship.

The rSWV reconstruction showed anomalies consistent with the instrumental precipitation record for 1901-1981 (Figure 3). In particular, the reconstruction correctly identifies the severe US nation-wide dust bowl era drought in the 1930s as well as the drought year 1956, the single worst drought year of the 1950s drought (Fye et al. 2003). However, when compared at a decadal scale after application of a 10-year smoothing spline, the rSWV reconstruction and instrumental record are less consistent before 1950 (Figure 5). This is likely a result of the changing variability in the reconstruction – in some

periods the reconstruction is quite variable as seen by the exaggerated response to extreme precipitation values, while in other periods there is less variability and this response is less exaggerated. This is indicative that the trees are either responding to a combination of other factors or are experiencing inconsistent lagged precipitation effects.

In years prior to the instrumental record, the rSWV reconstruction identifies several dry periods in 1760-1776, 1867-1874, and 1894-1902. There is evidence of a dry period from 1884-1902 in the NADA, JT, and MP reconstructions. The other dry periods are less pronounced in the compared drought or precipitation reconstructions, or are not apparent.

The rSWV reconstruction shows an 11-year cyclicity (Figure 6), a periodicity that has been observed in both instrumental and paleo-reconstructed temperature and moisture indices, such as the Northern Hemisphere annual average land air temperature record extending from 1951-1980, the Northern Hemisphere annual temperature anomalies reconstructed from proxy data for 1579-1880, as well as for many of the contiguous states using state-averaged instrumental temperature and precipitation records (Hancock & Yarger 1979, Lassen & Friis-Christensen 1995). In particular, this cyclic pattern has been identified in June precipitation in the southeastern US (Hancock & Yarger 1979), but was not apparent in western US tree-ring based PDSI reconstructions (Cook et al. 1997). This observed 11-year periodicity is a characteristic of the solar cycle, which is reflected in terrestrial climate, and identified as one of the contributing factors that determine global temperature (Lassen & Friis-Christensen 1995, Reid 2002, National Research Council 1994). Solar periods of high and low activity can be measured by the number of sunspots or the solar cycle length (Friis-Christensen & Lassen 1991, Usoskin et al. 2003). A larger number of sunspots indicates greater solar activity, and the magnetic fields in these sunspots have the ability to release large amounts of stored energy as solar flares or coronal mass ejections. These changes in released energy in turn affect the realized weather patterns. Studies have

shown that these changes in released energy may also influence hydroclimate (Hancock & Yarger 1979, Nichols & Huang 2012). However, despite the presence of strong correlations between terrestrial climate records and solar cycles, physical mechanisms that explain the effects of external solar forcing on global circulation patterns have yet to be fully understood (Franks 2002).

We have shown that QUPR growth in the southern Appalachians is positively influenced by early summer precipitation and we successfully reconstructed May-June precipitation for the period 1750-1981 and thus extended the instrumental record by150 years. Long records of climatic variability and its influence on ecosystems are particularly important in the Southern Appalachians, one of the most biologically diverse temperate forest systems. Extending the climate record will allow scientists to have more information as to how climate affects tree growth and shapes ecosystems. This will better prepare us for predicting future vegetation changes that may occur with a changing climate. This region has supported continuous forest communities longer than any other area on the North American continent, and hosts many rare, endemic species (NCNHP 2012). Additionally, it harbors many disjunct species populations. The southern Appalachians also provide ecosystem services such as carbon storage, watershed and water quality protection, and serve as a timber source (Zipper et al. 2011). Understanding past climate-ecosystem relationships in this region will enable scientists and landowners to better manage natural resources in our current changing climate.

5 Acknowledgements

The authors would like to thank the North American Dendroecological Fieldweek (NADEF) Dendroclimatology group for assisting with data collection, and Carolyn Copenheaver for assisting with site selection. We would also like to thank the organizers of NADEF, especially Jim Speer.

391

Chron	Lat (N), Long (W)	SIC	MS	N	MSL	mjPR	jjPDSI	Period	Citation
BM	37.37, 80.24	0.556	0.208	76	128.3	0.50*	0.55*	1845 - 2010	This study
LH	35.62, 85.43	0.609	0.171	19	181.4	0.55*	0.48*	1750 - 1997	Stahle, D.W. & Therrell, M.D. 2005
WD	38.50, 78.35	0.523	0.163	26	250.8	0.43*	0.59*	1735 - 1981	Cook, E.R. 1994
CC	37.35, 80.37	0.592	0.218	20	194.1	0.38*	0.50*	1800 - 2001	Copenheaver, C.A. 2010
OC	39.88, 76.40	0.575	0.169	18	260.2	0.24**	0.19	1745 - 1981	Cook, E.R. 1994

392

393 Table 1: Site-specific details for the Brush Mountain (BM), Lynn Hollow (LH), Watchdog Mountain
394 (WD), Craig Creek (CC), and Otter Creek (CC) sites, including location, series intercorrelation (SIC),
395 mean sensitivity (MS), number of series (N), mean segment length (MSL), correlations between the
396 chronology with both the averaged May-June precipitation (mjPR) and averaged June-July PDSI
397 (jjPDSI), the period for which the EPS is greater than 0.85, and the data citation. All correlation
398 statistics between the chronologies and the weather data were significant ($p < 0.01$ indicated by *, $p <$
399 0.05 indicated by **), except for one ($p = 0.19$).
400
401
402
403

404

Site	Location	Variable	Range (years)	Data type	Variance explained (R^2) [A]
NADA [11]	37° 30' N, 80° 0' W VA	Jun-Aug PDSI	1185-2006	Tree rings	0.55*
JT [35]	Coastal NC and VA	July PDSI	1700-1984	Tree rings	0.44
NC [36]	Statewide NC	Apr-Jun precip	933-1985	Tree rings	0.54
SC [36]	Statewide SC	Mar-Jun precip	1005-1985	Tree rings	0.58
GA [36]	Statewide GA	Mar-Jun precip	933-1985	Tree rings	0.68
MP [37]	38° 13' N, 78° 10' W; VA	Early summer precip	1784-1966	Tree rings & Meteorological diary	0.39

405

406 [A] R^2 values as reported in cited references; may or may not be adjusted.

407 * Median value of R^2 for all gridpoints in the PDSI reconstruction grid (see [11]).

408

409 Table 2: Details for the six southeastern US moisture reconstructions compared to the southwest
410 Virginia reconstruction (rSWV).

411

	Calibration			
	mjPR		jjPDSI	
	1901-1941	1942-1981	1901-1941	1942-1981
RE	0.10 (0.20)	0.30 (0.42)	0.44 (0.26)	-0.41 (-0.66)
CE	0.10 (0.19)	0.30 (0.41)	0.39 (0.20)	-0.60 (-0.88)
Calibration R^2	0.64 (0.75)	0.56 (0.55)	0.58 (0.62)	0.74 (0.59)
Verification R^2	0.56 (0.55)	0.64 (0.75)	0.74 (0.59)	0.59 (0.62)

Table 3: PCA_{1845} and SWV (or $PCA_{1750;}$ in brackets) reconstruction skill statistics for average May-June precipitation (mjPR) and average June-July PDSI (jjPDSI). Statistics include the reduction of error (RE), coefficient of efficiency (CE), and the calibration and verification period R^2.

425
426

	Recon	PDSI			Precip		
	rSWV	JT	NADA	NC	SC	GA	MP[A]
rSWV	1						
JT	0.215*	1					
NADA	0.593*	0.502*	1				
NC	0.227*	0.396*	0.424*	1			
SC	0.118	0.178*	0.352*	0.581*	1		
GA	0.079	0.196*	0.345*	0.474*	0.766*	1	
MP[A]	0.378*	0.288*	0.499*	0.132	0.090	0.109	1

427
428 Table 4: Annual correlation (1750-1981) between the southwest Virginia reconstruction (rSWV) and
429 other reconstructions including the NADA and JT drought reconstructions; and the NC, SC, GA, and
430 MP precipitation reconstructions. All values indicated by * indicate significant correlations at the $p <$
431 0.01 level.
432 [A] Reconstruction covers only the period 1764 - 1966.
433
434

435 Figure 1: Regional chronology sample locations.

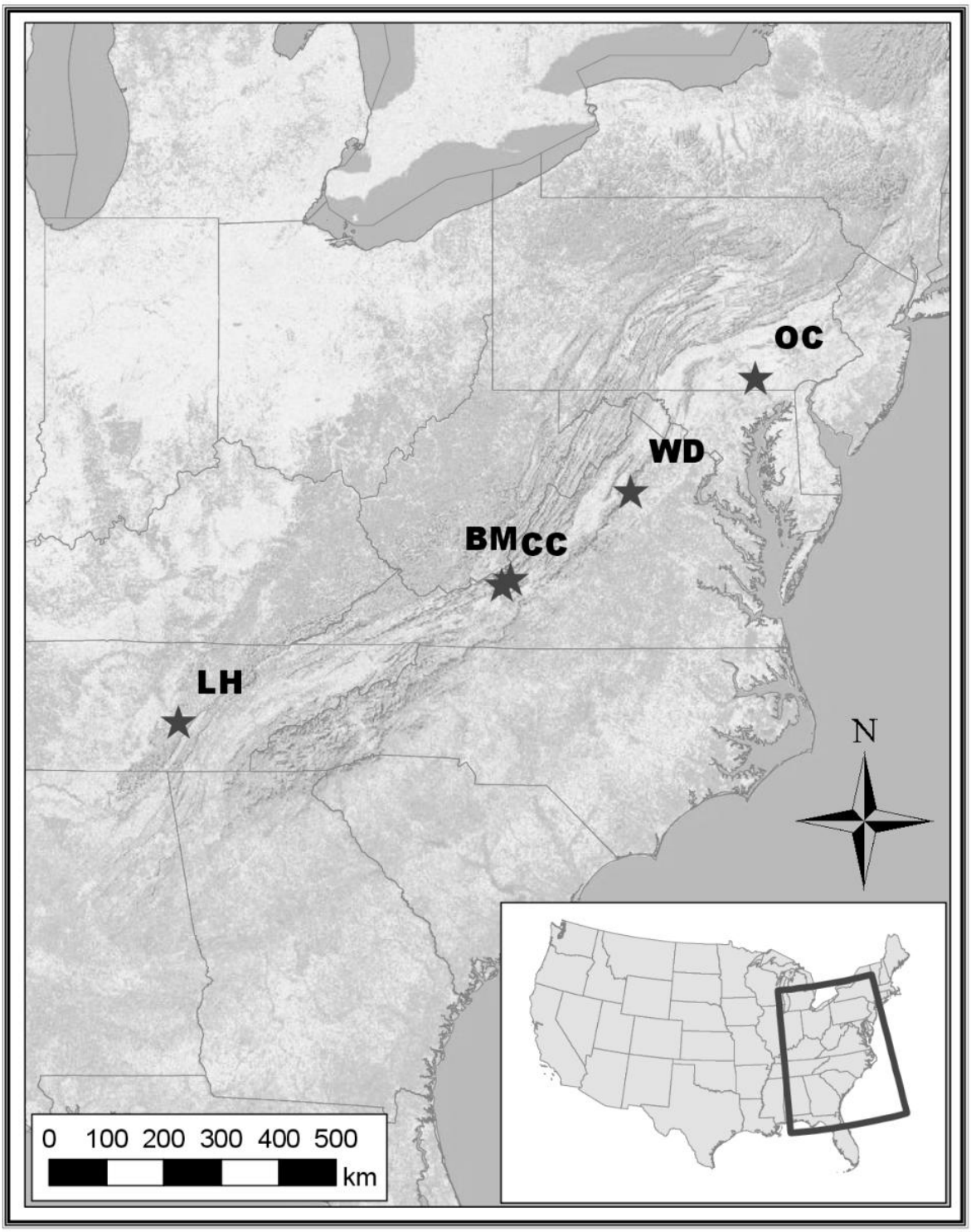

436

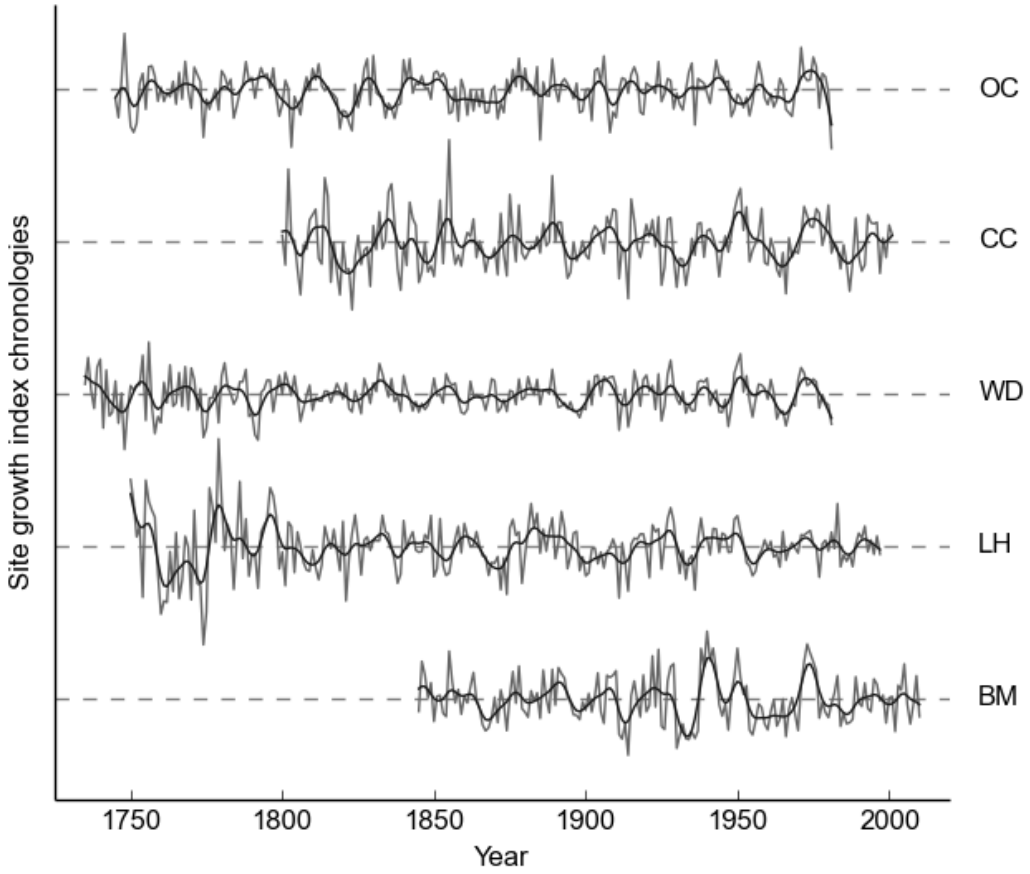

437

438 Figure 2: The five chronologies used in PCA_{1850}. The chronology built from the sample data at Brush
439 Mountain (BM) appears at the bottom, while the others are the regional chronologies from Lynn
440 Hollow (LH), Watchdog Mountain (WD), Craig Creek (CC), and Otter Creek (OC).

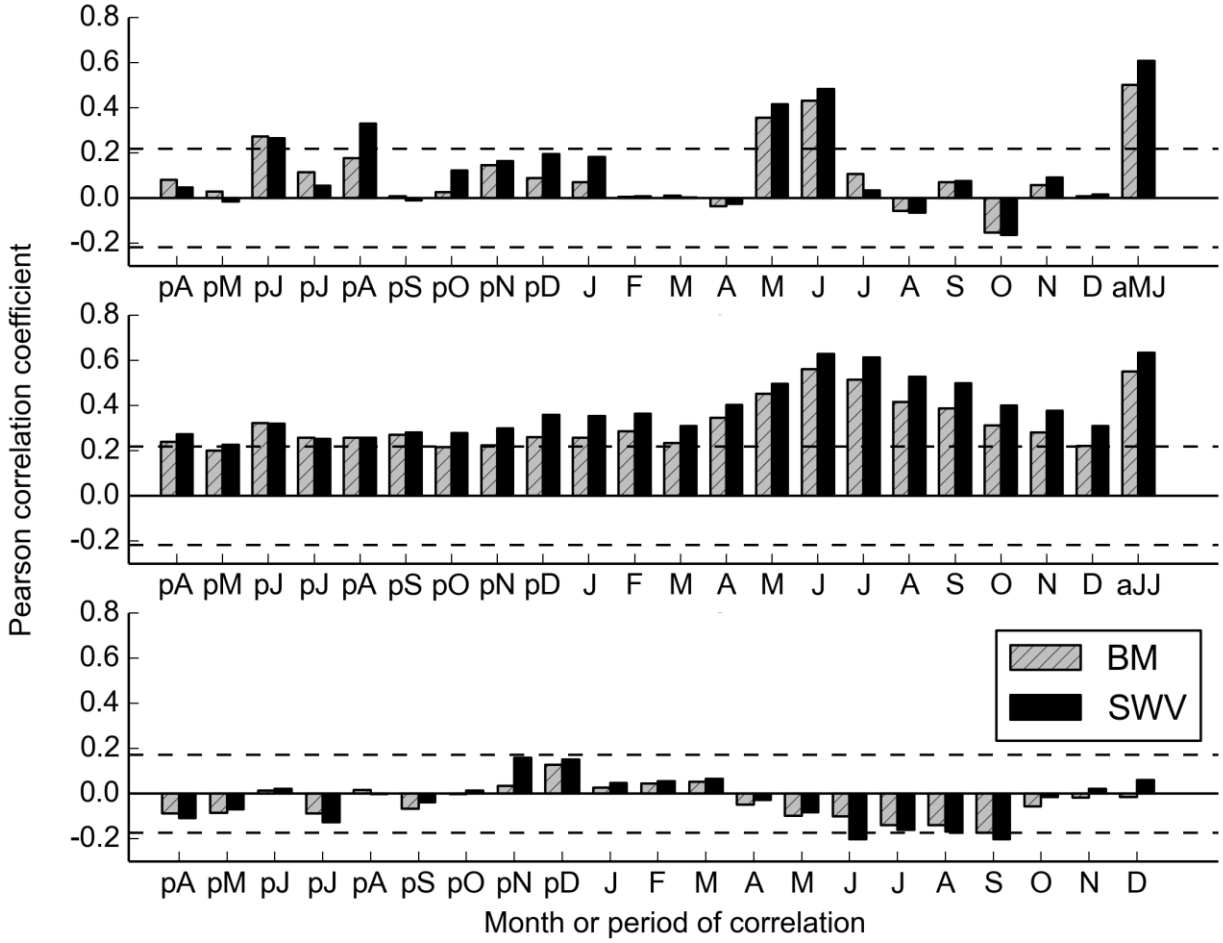

441

442 Figure 4: Correlation between the Bruch Mountain (BM) and southwest Virginia (SWV) chronologies
443 and the gridded (Top) monthly precipitation from previous April (pA) through December (D) as well
444 as for average May and June (aMJ); (Center) average PDSI from previous April (pA) through
445 December (D) as well as for average June and July (aJJ); and (bottom) average monthly temperature
446 from previous April (pA) through December (D).

447

448

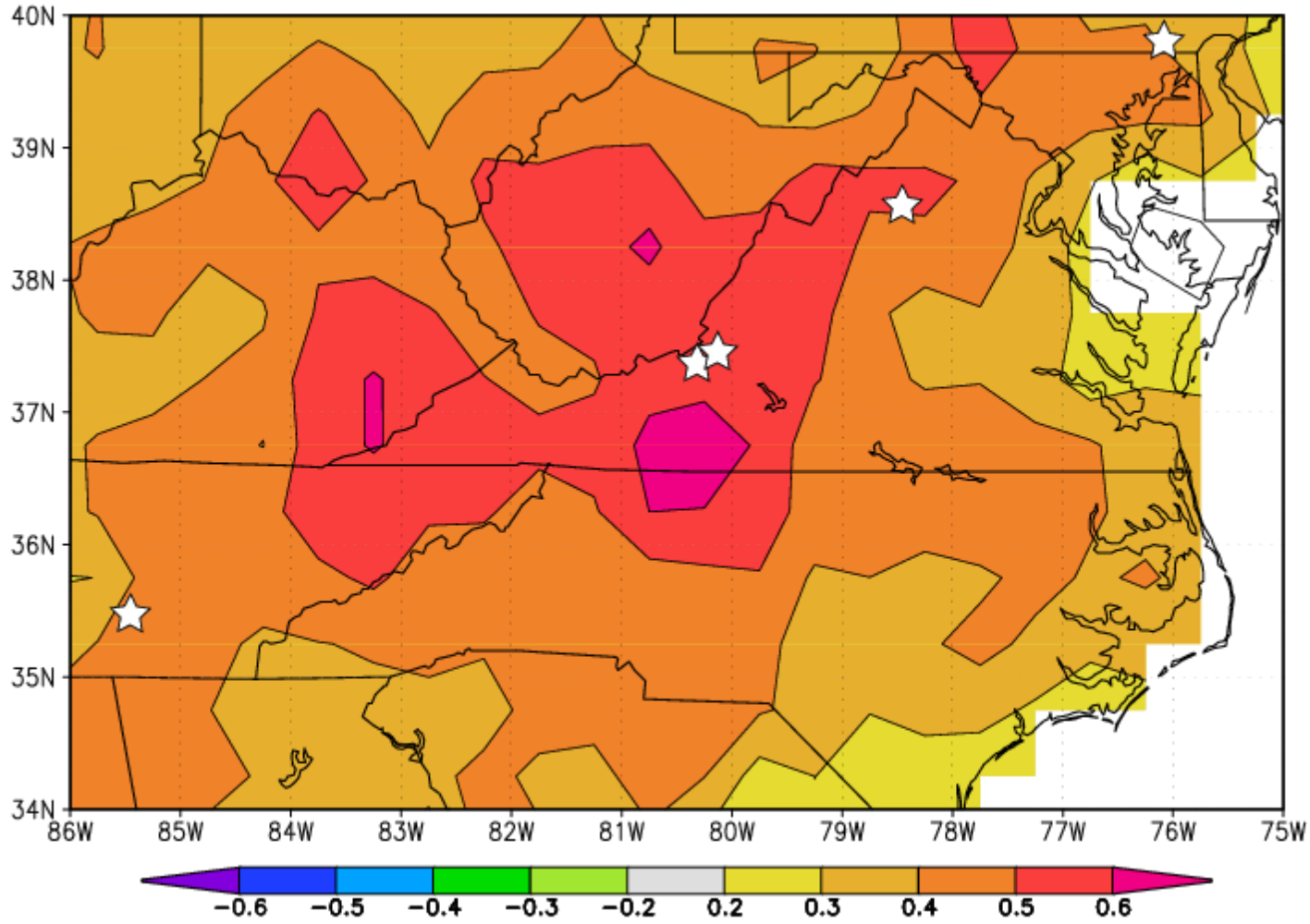

Figure 3: Correlation map (1901-1981) between the southwest Virginia chronology (SWV) and gridded average May-June precipitation (CRUTS3.10). Stars indicate the sample sites of the chronologies included in the nested principal component analysis resulting in the growth series extending from 1750-1981 (PCA_{1750}).

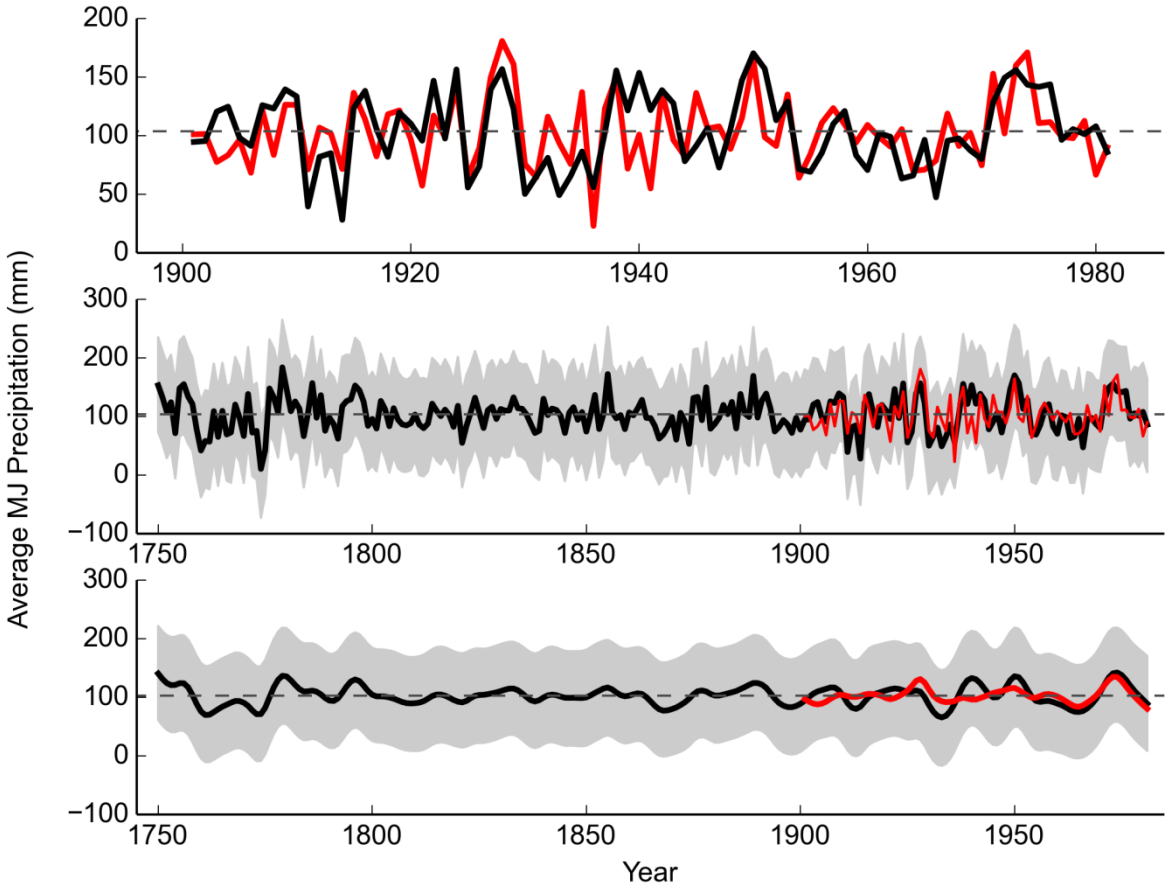

Figure 5: Top panel: southwest Virginia reconstruction (rSWV, black curve) and the average May-June precipitation (red curve; 1901-1981). Middle panel: rSWV reconstruction (black curve), 95% credibility interval (shaded grey area), and average May-June precipitation (red curve) for the 1750-1981 period of reconstruction. Bottom panel: Smoothed (10-year) rSWV reconstruction (black curve), 95% credible interval (shaded grey area), and average May-June precipitation (red curve). Smoothing performed using a 10-year smoothing spline to highlight decadal-scale variability.

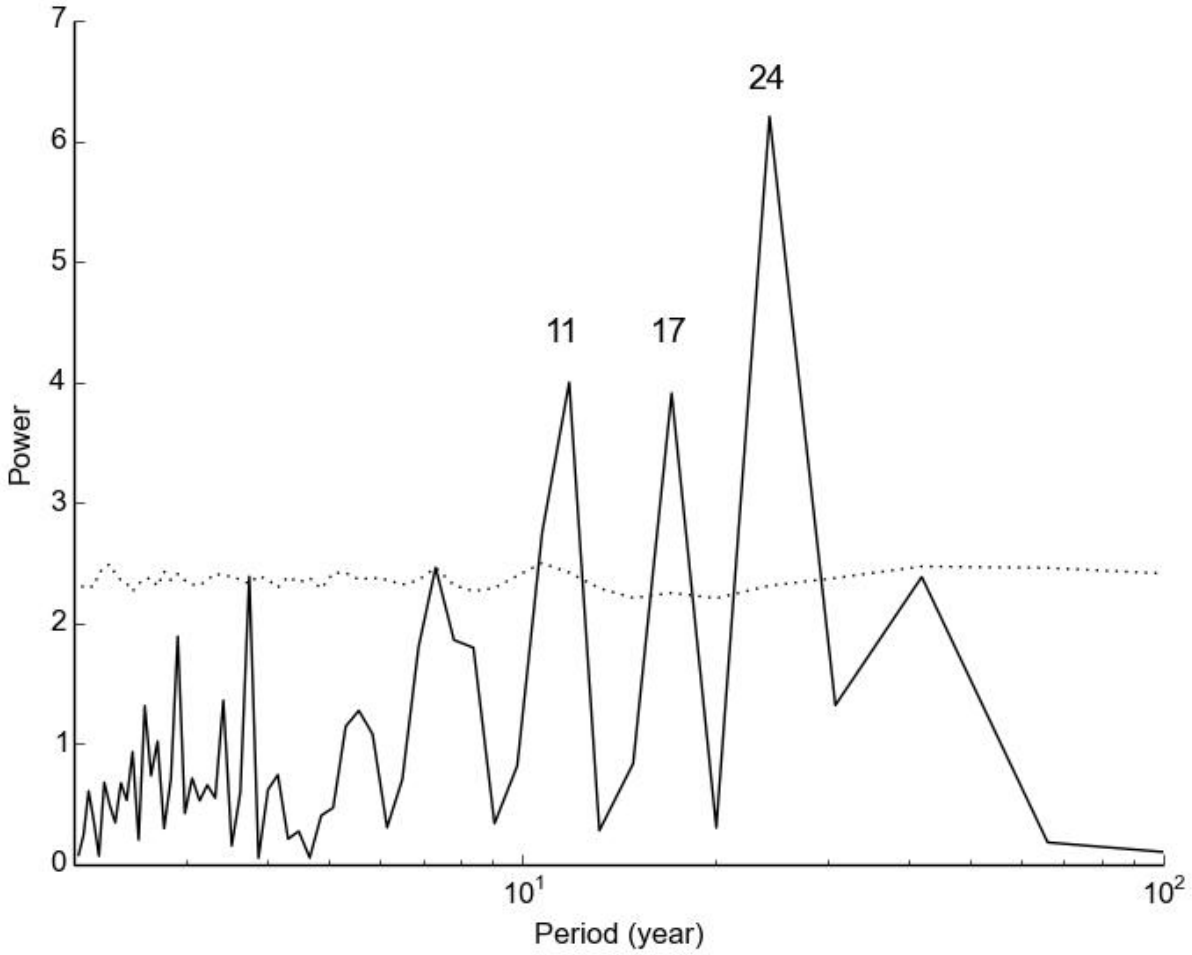

466

467 Figure 6: Periodogram of the southwest Virginia reconstruction (rSWV) showing spectral power peaks
468 at approximately 11, 17, and 24 years.

469

470

471

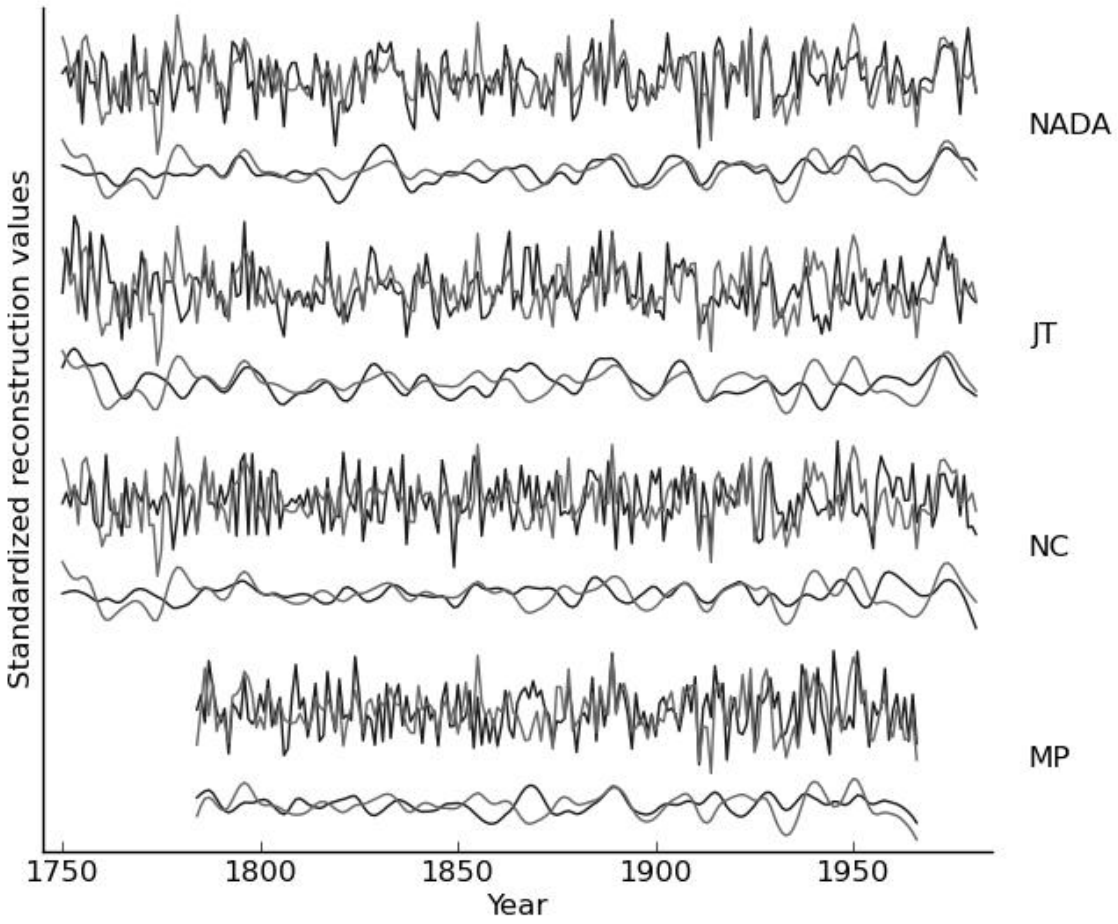

472

473

474 Figure 7: The standardized average May-June precipitation southwest Virginia reconstruction (rSWV,
475 grey lines) is plotted on top of the other moisture reconstructions (NADA, JT, NC, and MP; black
476 lines) which were significantly correlated to rSWV. Standardized reconstructions are shown at an
477 annual scale and at a decadal-scale obtained by application of a 10-year smoothing spline. Particularly
478 notable differences between rSWV and the other reconstructions are the year 1774 and the interval
479 1863-1872.

480

481

References

Anchukaitis KJ, Evans MN, Kaplan A, Vaganov EA, Hughes MK, Grissino-Mayer HD, Cane MA (2006) Forward modeling of regional scale tree-ring patterns in the southeastern United States and the recent influence of summer drought. *Geophysical Research Letters* 33(4):L04705

Beniston M, Diaz HF, Bradley RS (1997) Climatic change at high elevation sites: an overview. *Climatic Change* 36(3):233–251

Büntgen U, Frank DC, Kaczka RJ, Verstege A, Zwijacz-Kozica T, Esper J (2007) Growth responses to climate in a multi-species tree-ring network in the Western Carpathian Tatra Mountains, Poland and Slovakia. *Tree Physiology* 27(5):689–702

Cole JE, Overpeck JT, Cook ER (2002) Multiyear La Niña events and persistent drought in the contiguous United States. *Geophysical Research Letters* 29(13):25–1.

Cook ER (1987) The decomposition of tree-ring series for environmental studies. *Tree-Ring Bulletin* 47:37–59

Cook ER (1985) A time series analysis approach to tree ring standardization. PhD dissertation, The University of Arizona, AZ

Cook ER, Woodhouse CA, Eakin CM, Meko DM, Stahle DW (2004) Long-term aridity changes in the western United States. *Science* 306(5698):1015–1018

Cook ER, Meko DM, Stahle DW, Cleaveland MK (1999) Drought reconstructions for the continental United States. *Journal of Climate* 12(4):1145–1162

Cook ER, Peters K (1997) Calculating unbiased tree-ring indices for the study of climatic and environmental change. *The Holocene* 7(3):361–370

Cook ER, Peters K (1981) The smoothing spline: a new approach to standardizing forest interior tree-ring width series for dendroclimatic studies. *Tree-ring bulletin* 41:45–53

Cook ER, Seager R, Cane MA, Stahle DW (2007) North American drought: reconstructions, causes, and consequences. *Earth-Science Reviews* 81(1):93–134

Cook ER, Meko DM, Stockton CW (1997) A new assessment of possible solar and lunar forcing of the bidecadal drought rhythm in the western United States. *Journal of Climate* 10 (6):1343–1356

Cook ER, Briffa K, Shiyatov S, Mazepa V (1990) Tree-ring standardization and growth-trend estimation. In: Cook ER, Kairiukstis LA (eds) *Methods of dendrochronology: applications in the environmental sciences*. Kluwer

Cook ER, Briffa HR, Jones PD (1994) Spatial regression methods in dendroclimatology: a review and comparison of two techniques. *International Journal of Climatology* 14(4):379–402

Dickson RE, Tomlinson PT (1996) Oak growth, development and carbon metabolism in response to water stress. In: *Annales des Sciences Forestières*, volume 53, p 181–196

Druckenbrod DL, Mann ME, Stahle DW, Cleaveland MK, Therrell MD, Shugart HH (2003) Late-eighteenth-century precipitation reconstructions from James Madison's Montpelier plantation. *Bulletin of the American Meteorological Society* 84(1):57–72

Friis-Christensen E, Lassen K (1991) Length of the solar cycle- an indicator of solar activity closely associated with climate. *Science* 254(5032):698–700

Fye FK, Stahle DW, Cook ER (2003) Paleoclimatic analogs to twentieth-century moisture regimes across the United States. *Bulletin of the American Meteorological Society* 84(7):901–909

Hancock DJ, Yarger DN (1979) Cross-spectral analysis of sunspots and monthly mean temperature and precipitation for the contiguous United States. *Journal of Atmospheric Sciences* 36:746–746

Fritts HC (2012) *Tree rings and climate*. Academic Press Inc, London, UK

Fritts HC, Guiot J, Gordon GA, Schweingruber F (1990) Methods of calibration, verification, and reconstruction. *Methods of Dendrochronology* p 163–217

Harris I, Jones PD, Osborn TJ, Lister DH (2014) Updated high-resolution grids of monthly climatic observations–the CRU TS3. 10 dataset. *International Journal of Climatology* 34(3):623–642

Holmes RL (1983) Computer-assisted quality control in tree-ring dating and measurement. *Tree-ring bulletin* 43(1):69–78

IPCC (2013) Climate Change 2013: The Physical Science Basis. Contribution of Working Group I to the Fifth Assessment Report of the Intergovernmental Panel on Climate Change. T.F. Stocker, D. Qin, G.-K. Plattner, M. Tignor, S.K. Allen, J. Boschung, A. Nauels, Y. Xia, V. Bex, and P.M. Modgley (eds)

IPCC (2007) Climate Change 2007: Synthesis Report. Contribution of Working Groups I, II and III to the Fourth Assessment Report of the Intergovernmental Panel on Climate Change. Pachauri RK and Reisinger A (eds).

Jacob GC, D'Arrigo R (1989) Reconstructed northern hemisphere annual temperature since 1671 based on high-latitude tree-ring data from North America. *Climatic Change* 14(1): 39–59

K. Kattenberg, F. Giorgi, H. Grassl, G.A. Meehl, J.F.B. Mitchell, R.J. Stouffer, T. Tokioka, A.J. Weaver, and T.M.L Wigley. Climate models–projections of future climate. In: J.T. Houghton, LG Meiro Filho, B.A. Callander, N. Harris, A. Kattenburg, and K. Maskell (eds) Climate change 1995: The science of climate change: contribution of working group I to the second assessment report of the Intergovernmental Panel on Climate Change, p 285–357.

Lassen K, Friis-Christensen E (1995) Variability of the solar cycle length during the past five centuries and the apparent association with terrestrial climate. *Journal of Atmospheric and Terrestrial Physics* 57(8):835–845

LeBlanc DC (1993) Temporal and spatial variation of oak growth-climate relationships along a pollution gradient in the midwestern United States. *Canadian Journal of Forest Research* 23 (5):772–782.

Li Y (2011) *Dendroclimatic Analysis of Climate Oscillations for the Southeastern United States from Tree-ring Network Data*. PhD dissertation, University of Tennessee, TN

Melvin TM, Briffa KR (2008) A "signal-free" approach to dendroclimatic standardisation. *Dendrochronologia* 26(2):71–86

Monserud RA (1986) Time-series analyses of tree-ring chronologies. *Forest Science* 32(2): 349–372

Nichols JE, Huang Y (2012) Hydroclimate of the northeastern United States is highly sensitive to solar forcing. *Geophysical Research Letters* 39(4)

National Oceanic and Atmosheric Administration (NOAA) Climate Prediction Center (2005) El Niño Southern Oscillation (ENSO). http://www.cpc.ncep.noaa.gov/products/precip/CWlink/MJO/enso.shtml (accessed Sept 2014)

North Carolina Natural Heritage Program (NCNHP) (1999) An Inventory of the Significant Natural Areas of Ashe County, North Carolina. http://www.ncnhp.org/Images/Ashe10-_10-_2005.pdf (accessed Sept 2014)

North GR, Biondi F, Bloomfield P, Christy JR, Cuffey KM, Dickinson RE, Druffel ERM, Nychka D, Otto-Bliesner B, Roberts N and others (2006) Surface temperature reconstructions for the last 2,000 years. NRC Statement to Subcommittee on Oversight and Investigations, Committee on Energy and Commerce, US House of Representatives.

National Research Council (NRC) (1994). *Solar Influences on Global Change*. The National Academies Press, Washington, DC

Oliver CD (1980) Forest development in North America following major disturbances. *Forest ecology*

and management 3:153–168

Pan C, Tajchman SJ, Kochenderfer JN (1997) Dendroclimatological analysis of major forest species of the central Appalachians. *Forest Ecology and Management* 98(1):77–87

Peters K, Jacoby GC, Cook ER (1981) Principal components analysis of tree-ring sites. *Tree-Ring Bulletin* 41:1–19

Phipps RL (1982) Comments on interpretation of climatic information from tree rings, eastern North America. *Tree-ring bulletin* 42:11–22

Pielke Jr RA, Landsea CN (1999) La Niña, El Niño and Atlantic hurricane damages in the United States. *Bulletin of the American Meteorological Society* 80(10):2027–2033

Reid GC (2002) Solar total irradiance variations and the global sea surface temperature record. Journal of Geophysical Research: Atmospheres (1984-2012) 96(D2):2835-2844.

Robertson PA (1992) Factors affecting tree growth on three lowland sites in southern Illinois. *American Midland Naturalist*, p 218–236

Rubino DL, McCarthy BC (2000) Dendroclimatological analysis of white oak (*Quercus alba* L., Fagaceae) from an old-growth forest of southeastern Ohio, USA. *Journal of the Torrey Botanical Society*, p 240–250

Seager R, Tzanova A, Nakamura J (2009) Drought in the southeastern United States: Causes, variability over the last millennium, and the potential for future hydroclimate change. Journal of Climate 22(19):5021–5045

Sobolowski S, Pavelsky T (2012) Evaluation of present and future North American Regional Climate Change Assessment Program (NARCCAP) regional climate simulations over the southeast United States. *Journal of Geophysical Research: Atmospheres (1984-2012)*, 117(D1)

Speer JH, Grissino-Mayer HD, Orvis KH, Greenberg CH (2009) Climate response of five oak species in the eastern deciduous forest of the southern Appalachian Mountains, USA. *Canadian Journal of Forest Research* 39(3):507–518

Stahle DW, Cleaveland MK (1992) Reconstruction and analysis of spring rainfall over the southeastern US for the past 1000 years. *Bulletin of the American Meteorological Society* 73(12) :1947-1961

Stahle DW, Cleveland MK (1993) Large-scale climatic influences on baldcypress tree growth across the southeastern United States. In: Jones PD, Bradley RS, Jouzel J (eds) *Climatic variations and forcing mechanisms of the last 2000 years*, NATO ASI , I41, p 125 – 140

Stahle DW, Cleaveland MK, Blanton DB, Therrell MD, Gay DA (1998) The lost colony and Jamestown droughts. *Science* 280(5363):564–567

Stokes MA, Smiley TL (1996) *An introduction to tree-ring dating*. University of Arizona Press, AZ

Torrence C, Compo GP (1998) A practical guide to wavelet analysis. *Bulletin of the American Meteorological society* 79(1):61–78

Trouet V, van Oldenborgh GJ (2013) KNMI Climate Explorer: a web-based research tool for high-resolution paleoclimatology. *Tree-Ring Research* 69(1):3–13

Usoskin IG, Solanki SK, Schüssler M, Mursula K, Alanko K (2003) Millennium-scale sunspot number reconstruction: Evidence for an unusually active sun since the 1940s. *Physical Review Letters* 91(21):211101

Wang, H, Fu, R, Kumar, A, Li, W (2010) Intensification of summer rainfall variability in the southeastern United States during recent decades. Journal of Hydrometeorology 11:1007-1018

Wigley TML, Briffa KR, Jones PD (1984) On the average value of correlated time series, with applications in dendroclimatology and hydrometeorology. *Journal of Climate and Applied Meteorology* 23(2):201–213

Wold S, Esbensen K, Geladi P (1987) Principal component analysis. *Chemometrics and intelligent laboratory systems* 2(1):37–52

Yamaguchi DK (1991) A simple method for cross-dating increment cores from living trees. *Canadian Journal of Forest Research* 21(3):414–416.

Zipper CE, Burger JA, Skousen JG, Angel PN, Barton CD, Davis V, Franklin JA (2011) Restoring forests and associated ecosystem services on Appalachian coal surface mines. *Environmental management* 47(5):751–765

Zweifel R, Zimmermann L, Zeugin F, Newbery DM (2006) Intra-annual radial growth and water relations of trees: implications towards a growth mechanism. *Journal of Experimental Botany* 57(6):1445–1459

631